

2023年度 11)SCOSTEP Visiting Scholar (SVS) Program (in ISEE) 目次詳細

2023 11)SCOSTEP Visiting Scholar (SVS) Program in ISEE List

7 件

*所属・職名は2024年3月現在
*Affiliation and Department displayed are current as of March 2024.

研究代表者 Principal Investigator	所属機関* Affiliation	所属部局 Department	職名* Job title	研究課題名 Project Title	頁 Page	備考 Remarks
George Ochieng Ondede	The Technical University of Kenya, Kenya	Department of Astronomy and Space Sciences	graduate-course student	The impact of Geomagnetic Storms on GNSS within the Low and Mid Latitude Sector During the 24th Solar Cycle.	301	
Akshay Shivaji Patil	Sanjay Ghodawat University, Kolhapur, India		graduate-course student	To study the variation in TEC scintillation during the propagation of Equatorial Plasma Bubbles (EPBs).	303	
Upadhyay Kshitiz	Physical Research Laboratory, Ahmedabad, India	Space and Atmospheric Sciences Division	graduate-course student	Interrelation between electron temperature and O(1D) emission intensity	305	
Lalitha G Krishnan	Vikram Sarabhai Space Centre, India	SPACE PHYSICS LABORATORY	graduate-course student	Space weather during initial phase of solar cycle 25 and its impact on thermosphere-ionosphere system at different latitudes	307	
Rajesh Kumar Barad	Indian Institute of Geomagnetism, India	UAS	graduate-course student	Study on the generation and evolution of equatorial plasma bubbles under extreme weather, space weather, and natural hazard events and their connections to the mid-latitude processes	309	
Manu Varghese	Institute of Space Sciences, Shandong University, China		graduate-course student	Association of peak intensity of all low latitude auroras and high latitude magnetic field data with the corresponding geomagnetic activity indices and solar wind-IMF parameters.	311	
Ardra K P	India			Large scale changes in the polar ionosphere during CME and CIR storms, its relation to Sub-Auroral Polarization Streams (SAPS) and particle precipitation	313	

Effects of Ionospheric Scintillation on GNSS Positioning in the Low Latitude Region of Africa at the close of the 24th Solar Cycle

Principal Investigator: George Ochieng Ondede

Affiliation: Technical University of Kenya, Nairobi, Kenya

Position: Faculty, Department of Astronomy and Space Sciences and a Ph D Student

Period of Stay in ISEE

I arrived at the ISEE on Friday 12th January 2024 and stayed till 29th March 2024.

Research Summary

Purpose of the Research

The purpose of the research was to investigate the effects of scintillations on GNSS positioning in the low latitude regions of Africa at the tail end of the 24th solar cycle using the RTKLIB positioning applications.

Methodology

The Global Navigation Satellite Systems (GNSS) data (in form of RINEX files) for the work was obtained from the SOPAC website. The locations of the receivers considered were within the dip equatorial region of Africa. The RINEX observation files obtained from the station were unzipped and then processed using the GPS-TEC application software developed at Institute of scientific Research, Boston College, USA. We use the method suggested by Pi et al., (1997) to determine ROTI:

$$ROTI = \sqrt{\langle ROT^2 \rangle - \langle ROT \rangle^2}$$

ROTI is a good indicator of the existence of ionospheric irregularities and $ROTI \geq 0.5$ indicates the occurrence of irregular ionospheric activities relevant to ionospheric scintillation. The GNSS positioning errors were determined using the RTKLIB application software, (Takasu, 2009).

Preliminary Results

The seasonal variations of scintillations were determined for the two years, 2019 and 2020, at the end of the 24th solar cycle. for contrast, the peak year, 2014, was also analyzed. The plots are given in Figures 1 and 2.

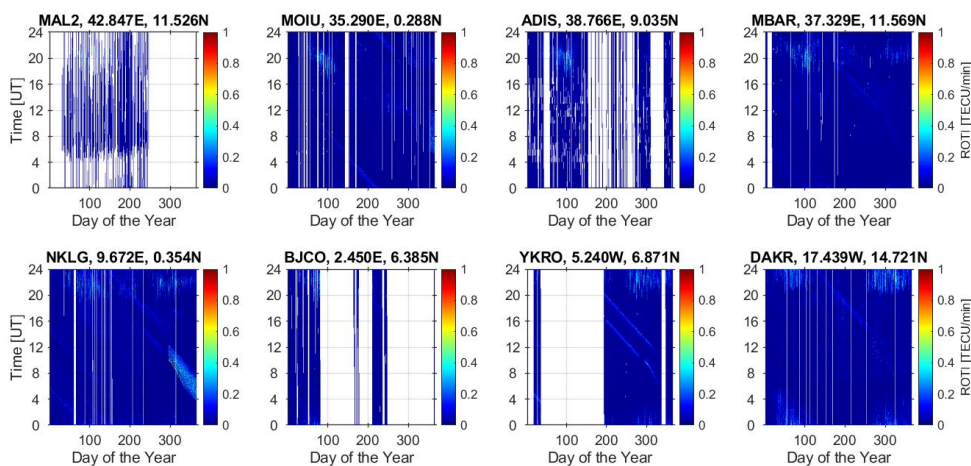


Figure 1: The time and seasonal variation of occurrences rate of ionospheric scintillation as observed by eight receivers within the dip equatorial region of Africa in the year 2019.

The data was observed to have a lot of data outages. The scintillations were also observed to be lower at the end of the 24th solar cycle compared to the period of the solar maximum. 2019 and 2020 represent the period of solar minimum. 2014, in Figure 2 represent the solar maximum for ease of comparison.

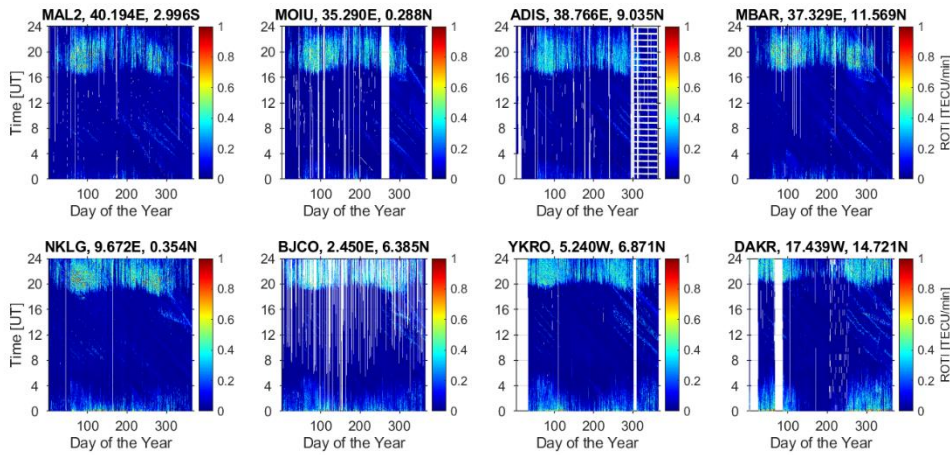


Figure 2: The time and seasonal variation of occurrences rate of ionospheric scintillation as observed by eight receivers within the dip equatorial region of Africa in the year 2014.

The ROTI was compared with the GNSS positioning errors. Figures 3 and 4 give summaries.

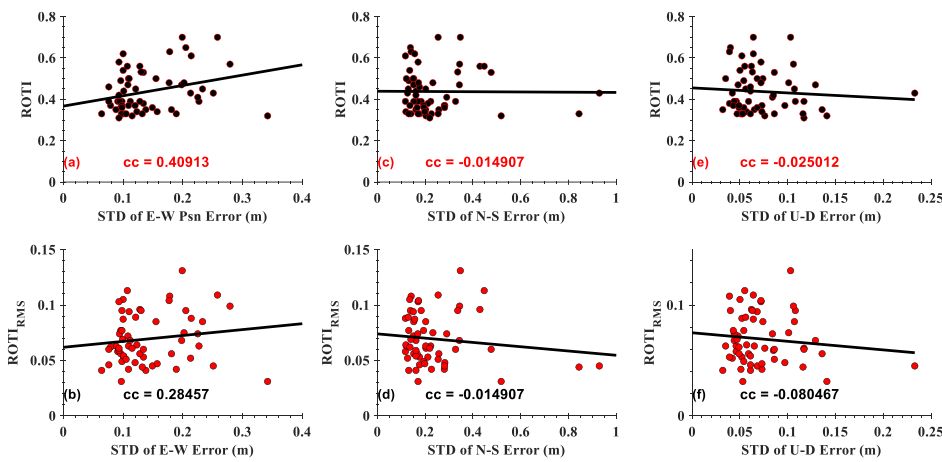
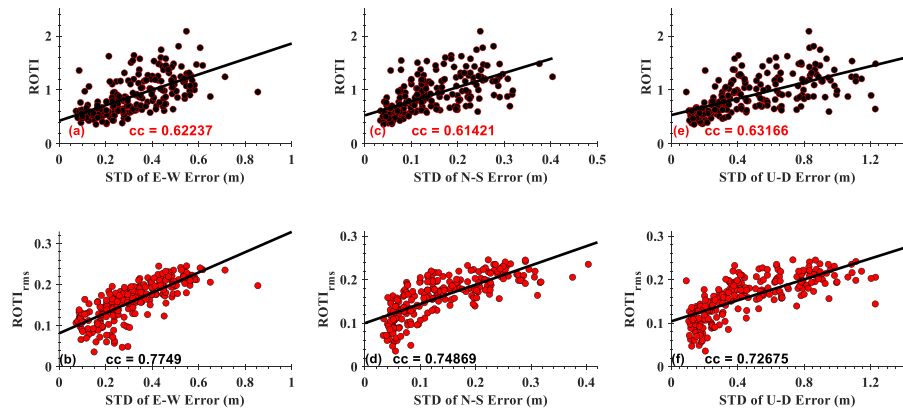


Figure 3: The plots showing positioning errors for all the days in 2019 for the receivers with $ROTI \geq 0.25$ in all the stations considered. The correlation coefficients are indicated as cc in each subplot.

Figure 4: Positioning errors for all the days with $ROTI \geq 0.25$ for Mbar in 2014. The correlation coefficients are indicated.



Summary

1. There was observed diurnal and seasonal variations of ionospheric scintillations.
2. During low solar activity period of the 24th solar cycle, 2019 and 2020, the magnitude scintillations could not trigger the GNSS positioning errors as opposed to the peak of the solar cycle, 2024.
3. The RTKLIB positioning application was found to be a useful tool for the determination of precise GNSS positioning errors.

The paper is yet to be sent for peer review as a process of publication.

Pi, X., Mannucci, A. J., Lindqwister, U. J., & Ho, C. M. (1997). Monitoring of global ionospheric irregularities using the worldwide GPS network. *Geophysical Research Letters*, 24(18), 2283–2286. <https://doi.org/10.1029/97GL02273>

Analysis of different techniques used to estimate impact of Equatorial Plasma Bubbles on Global Navigation Satellite System (GNSS) signals.

Mr. Akshay Patil, Sanjay Ghodawat University India, Ph.D. Student

Period of stay at ISEE: From 02 Oct. 2023 to 28 Dec. 2023.

Research summary:

In satellite-based navigation and positioning, ionospheric delay is regarded as a critical error source. Receivers on ground station with the help of satellite are used to determine the position, velocity and time information independently. In low latitudes, ionospheric variability significantly impacts positioning accuracy of GNSS signal. This necessitated the enhancement of precision and integration of many available satellite navigation systems.

Purpose: The existence of ionospheric abnormalities that may prevent continuous GNSS functioning, particularly in the Global positioning system (GPS) L2 frequency, is one of the primary issues in ionospheric modelling since, signals transmitted at L2 frequency are more susceptible to ionospheric delays compared to L1 frequency. Different estimation techniques have been developed over the time. Each of these techniques provides different aspect to ionosphere-radio frequency interaction. The main goal of this work is to analyse various estimation techniques to better understand the impact of ionospheric anomaly on GNSS signals.

Methods:

We have used two stations closely located in India as Base Station: LCK3 (26.9121° N , 80.9556° E) & Rover station: LCK4 (26.9140° N, 80.9588° E) for this event. Then we selected an event where Plasma bubble is detected (15th Jan 2022). To analyze this plasma bubble we have plotted Rate of Change TEC Index (ROTI) of that day and to analyze GNSS signal we used RTKLIB software.

RTKLIB: Among many GNSS data processing software, RTKLIB is an open-source program for GNSS positioning. Numerous common data formats, including RINEX OBS/NAV, BINEX, ANTEX, and IONEX, are supported by RTKLIB. RTKPLOT is used to visualize the solutions; it can display the number of satellites utilized in the computation, the position, and the ground track of the observation points. There are differences in the GNSS data utilized for post processing. First, a RINEX observation file from a GNSS receiver that serves as a base station and has a ".o" extension is used. The position of the rover station, which is made up of additional observation data, must be calculated. GNSS sites offer navigation files in addition to observation data. An output file ending in ".pos" is what RTKPOST produces. The positioning mode, statistically predicted accuracy, and various computational limitations are all detailed in the output file.

ROTI: Total electron content (TEC) is one of the most often utilized GNSS-based measures defining the ionospheric plasma density. We calculated ROTI using a running window for 5-min sets of ROT observations.

Results:

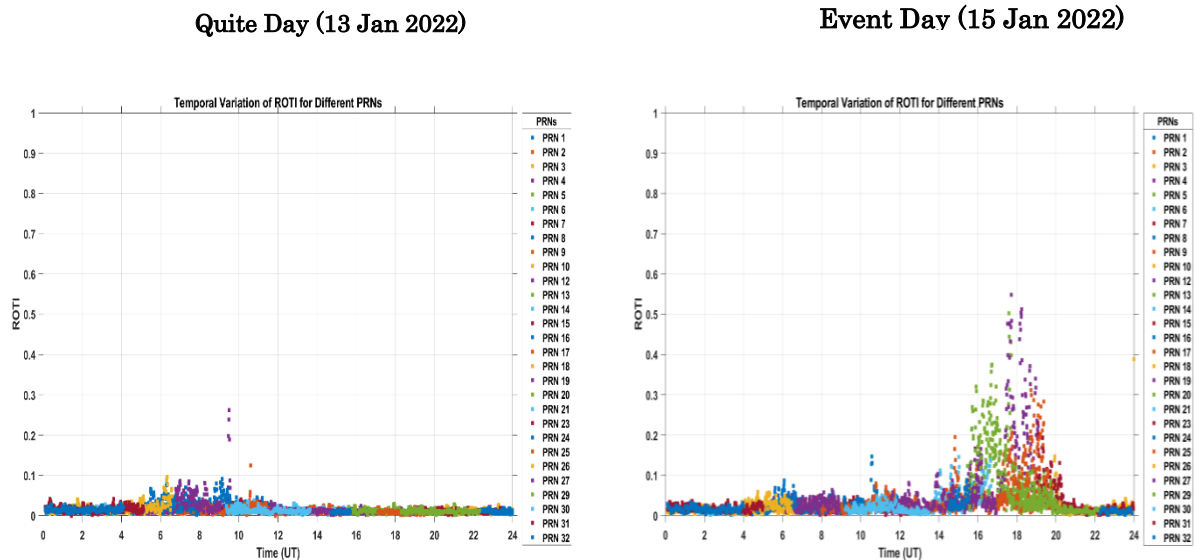


Fig.1 ROTI plot of base station LCK3 on quiet and event day.

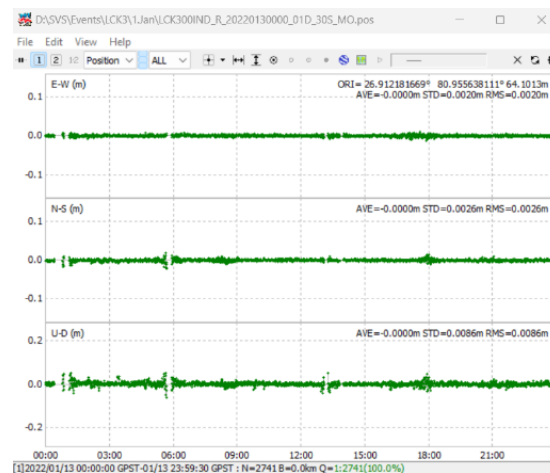


Fig. 2 shows variation in GNSS signal using DGNSS technique.

Our results shows that DGNSS (Code - based differential GNSS) provide best output for error detection in GNSS signal due to plasma bubble activity. We observed that after the occurrence of plasma bubble there is slight positioning error in GNSS signal. It also shows that meridional variation in positioning is slightly higher than that of zonal variation in positioning. But the error shows in this method is very minimum and it can be caused by other parameters. Hence to establish a solid relation multiple events at multiple station needs to be studied.

Interrelation between electron temperature and O(¹D) emission intensity

Mr. Kshitiz Upadhyay

Physical Research Laboratory, Ahmedabad, India

PhD Research Scholar

I, Kshitiz Upadhyay, a PhD student at Physical Research Laboratory, Ahmedabad, India visited the ISEE, Nagoya, Japan from Oct 01st to Dec 29th, 2023 under the SCOSTEP Visiting Scholar (SVS)-2023 program. The purpose of the visit was to perform the research work based on the investigations of night time atomic oxygen OI 630.0 nm emission intensity and the corresponding electron temperature variation for a mid-latitude phenomenon, known as Stable Auroral Red (SAR) arcs. In this work, the measurements of SAR arc emission intensities over Athabasca (Canada) and conjugate electron temperature (T_e) from DMSP for the events of year 2015 and 2018 observed by Gololobov et al., 2023 were utilized. As Gololobov et al., 2023 found a positive correlation between electron temperature and 630.0 nm emission intensities, we used these measured electron temperature and emissions to obtain the required plasmaspheric heat flux for the production of night time SAR arc emissions using a physics-based model, GLOW (Solomon, 2017). We further used these GLOW model obtained energy fluxes to estimate the electron densities using the Maxwell-Boltzmann's energy distribution function (MBF) and a comparison was made with DMSP measured electron densities. The results on estimated heat flux using measured emission and temperatures were found to match well as reported earlier by Kozyra et al., 1997, which were based on theoretical studies.

Apart from SAR arc studies, a partial work based on OI 630.0 nm nightglow emission intensities was also carried out during the stay at ISEE. These nightglow emissions were obtained using OMTI all-sky imager at Tromsø (Norway) for geomagnetically quiet days. In addition to observed nightglow emissions, GLOW model was also used to estimate the intensities of these emissions by providing measured electron density profiles from collocated EISCAT radar. The results obtained by the comparison of observed and estimated nightglow intensities over zenith suggested the occurrence of low-energy particle precipitation from plasma sheet region to the equatorward boundary of nightside auroral oval during geomagnetically quiet times. These results on low-energy transfer evident by OI 630.0 nm nightglow emissions also indicate towards the importance of magnetosphere-ionosphere coupling phenomena at high-latitudes during quiet periods of geomagnetic activity.

References

- Gololobov, A., Shiokawa, K., Baishev, D., Inaba, Y., Otsuka, Y., & Connors, M. (2023). Multi-event conjugate measurements of the SAR arc detachment from the auroral oval using DMSP satellites and an all-sky camera at Athabasca, Canada. *Journal of Geophysical Research: Space Physics*, e2022JA030544.
- Kozyra, J. U., Nagy, A. F., & Slater, D. W. (1997). High-altitude energy source (s) for stable auroral red arcs. *Reviews of Geophysics*, 35(2), 155-190.
- Solomon, S. C. (2017). Global modeling of thermospheric airglow in the far ultraviolet. *Journal of Geophysical Research: Space Physics*, 122(7), 7834-7848.

Space weather during initial phase of solar cycle 25 and its impact on thermosphere- ionosphere system at different latitudes

Lalitha G Krishnan,
Space Physics Laboratory,
Vikram Sarabhai Space Centre,
Thiruvananthapuram, India
Senior Research Fellow

As part of SCOSTEP Visiting Scholar (SVS) program -2023, I got the opportunity to visit Institute for Space Earth Environmental Research (ISEE), Nagoya University, Japan and work under the supervision of Prof. Kazuo Shiokawa for the period 01 October-29 December 2023. The aim was to study the impacts of the geomagnetic storms of different intensities in the rising phase of the solar cycle 25 on ionosphere-thermosphere system from high to equatorial latitudes in the Indian longitude sector. During the events of geomagnetic storms, the dynamo region electric field in the equatorial ionosphere, which generally is in the eastward direction, is altered by two processes: Prompt Penetration Electric Field (PPE) or/and Disturbance Dynamo Electric Field (DDE). PPE is the mapping of interplanetary electric field to the E-region ionosphere, which is an instantaneous effect and DDE is the alteration in the electric field caused due to the change in the global wind pattern caused by the intense joule heating in the auroral region, which takes few hours to manifest over the equatorial latitudes.

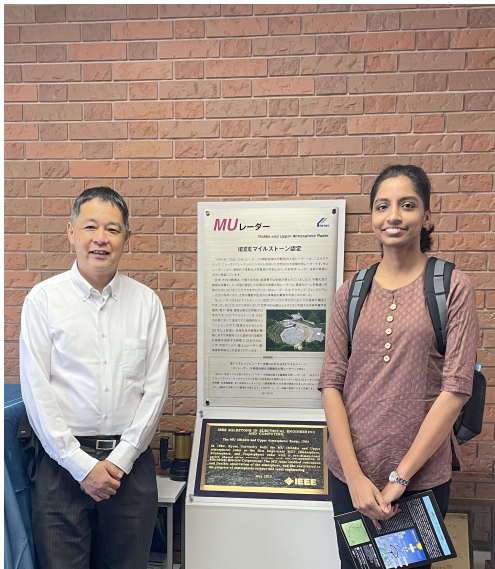


Photo taken with Prof. Shiokawa during the visit to Shigaraki MU radar observatory.

The drift of plasma irregularities in the ionospheric E-region is the best obtainable proxy for the estimation of dynamo electric field as there are no direct measurements available. The anomalous variation in the drift observed by 18MHz coherent, pulsed, monostatic HF radar at Thumba during 12 October 2021 and 28 November 2022 are found to be purely due to the mapping of the Interplanetary Electric Field (IEF_y) to the equatorial ionosphere as PPE, which is also supported by the Equatorial Electrojet (EEJ) strength over the location. The geomagnetic storm that occurred due to a Coronal Mass Ejection (CME) from the sun during April 2023 is by far the strongest storm of solar cycle 25 in terms of the SYM-H index. Its effects on the equatorial region as well as low

latitudes were studied. The work was commenced by pondering about the source of the anomalously high electron density over Thumba (8.5°N, 77°E and dip lat.= 1.96°N). The GPS- Total Electron Content (TEC) observations from different locations in India reveal the presence of Travelling Ionospheric Disturbances (TIDs) from north to south over the region. TEC data from ISEE database reveals the presence of TIDs that travel from north to southern hemisphere crossing the equator. The TIEGCM simulation of meridional wind and temperature with data assimilation by Assimilative Mapping of Ionospheric Electrodynamics (AMIE) technique was done in collaboration with Dr. Gang Lu, High Altitude Observatory (HAO), USA. The model output also shows the propagation of Travelling Atmospheric Disturbances (TADs). The manuscripts on the results obtained from the work carried out at ISEE are under preparation and will be soon communicated to a reputed journal.

During the visit to Nagoya, I had a chance to visit the MU Radar observatory, Shigaraki and witness the radio and optical facilities available for the probing of the Ionosphere-Thermosphere System.

Temporal Analysis of MSTID Impact on GNSS Positioning in Japan for 2022-2023

Rajesh Kumar Barad^{1,2}, Yuichi Otsuka²

¹Indian Institute of Geomagnetism, Navi Mumbai, India

²Institute for Space-Earth Environmental Research, Nagoya University, Nagoya, Japan

Purpose of this study

This study aims to conduct a comprehensive statistical analysis of the impact of Medium-scale traveling ionospheric disturbances (MSTIDs) on Global Navigation Satellite Systems (GNSS) positioning, utilizing observations from ground based GNSS receivers. The specific objective is to investigate the statistical distribution of MSTID-induced ranging errors and their impact on GNSS positioning accuracy under different ionospheric conditions over Japan.

Methods

This study investigates the effects of MSTIDs on the accuracy of GNSS positioning across the Japanese islands. To achieve this dual-frequency GPS datasets were collected from a vast network (GPS Earth Observation Network (GEONET)) of over ~1300 GNSS receivers in Japan. These datasets, sampled at a high temporal resolution of 30 seconds, provided the necessary foundation for identifying MSTIDs through their characteristic signatures in TEC observations. The rate of TEC index (ROTI) was computed to quantify the associated ionospheric disturbances, providing a crucial metric for subsequent analysis. The positioning errors induced by MSTIDs were evaluated using the open-source software RTKLIB. At its core, RTKLIB leverages the raw data obtained from various GNSS constellations, including GPS, GLONASS, Galileo, BeiDou, SBAS, and QZSS. One of the key strengths of RTKLIB lies in its support for a wide range of positioning modes. These modes include Single, DGPS/DGNSS, Kinematic, Static, Moving-Baseline, Fixed, PPP-Kinematic, PPP-Static, and PPP-Fixed. However, for the purposes of this study, the highly accurate kinematic relative positioning approach was selected. To facilitate a systematic regional examination, the Japanese islands were divided into five distinct latitudinal regions (Figure 1). To execute the relative positioning calculations, pairs of stations within close proximity (ranging from 5 to 15 km apart) were carefully identified within each region. These regions are represented by the green rectangles in Figure 1. From each station pair, one station was designated as the base station (marked by red triangles), while the other served as the rover station (green triangles), facilitating the relative positioning computations.

Results

This study investigated the impact of MSTIDs on GNSS positioning accuracy in Japan, focusing on events occurring on July 3, 2022, and July 2, 2023. Utilizing 2D detrended TEC maps sourced from GEONET, MSTID fronts were identified, characterized by northwesterly to southeasterly orientations propagating from the northeast to the southwest during summer nighttime hours. The study assessed potential GNSS positioning errors induced by MSTIDs across different latitudinal extents of Japan. Observation files from base and rover stations were processed to derive relative positioning, revealing variations in ROTI values and positioning errors across different regions. Notably, regions closer to the northernmost part of Japan exhibited minimal MSTID-induced positioning errors, while southern regions experienced escalating ROTI (~0.2-0.5 TECU/min) and positioning error values (~0.1-1 m), with region 3 being particularly susceptible to MSTID influence (Figure 2). Furthermore, regions 4 and 5, situated even further south, demonstrated heightened errors

attributed to equatorial and low-latitude phenomena, overshadowing the influence of MSTIDs.

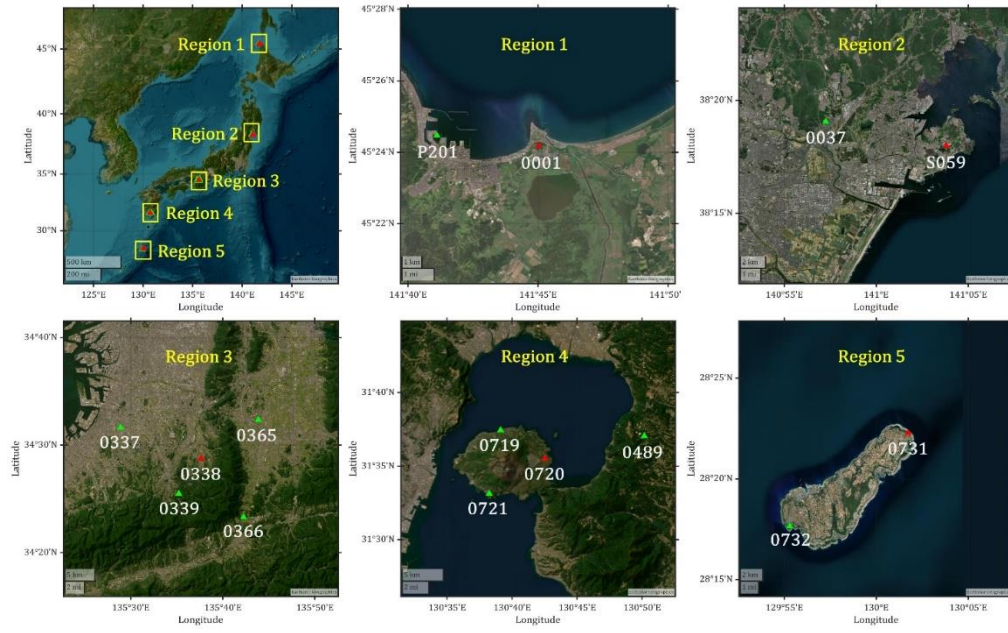


Figure 1: Spatial distribution of base and rover stations across various regions of the Japanese islands.

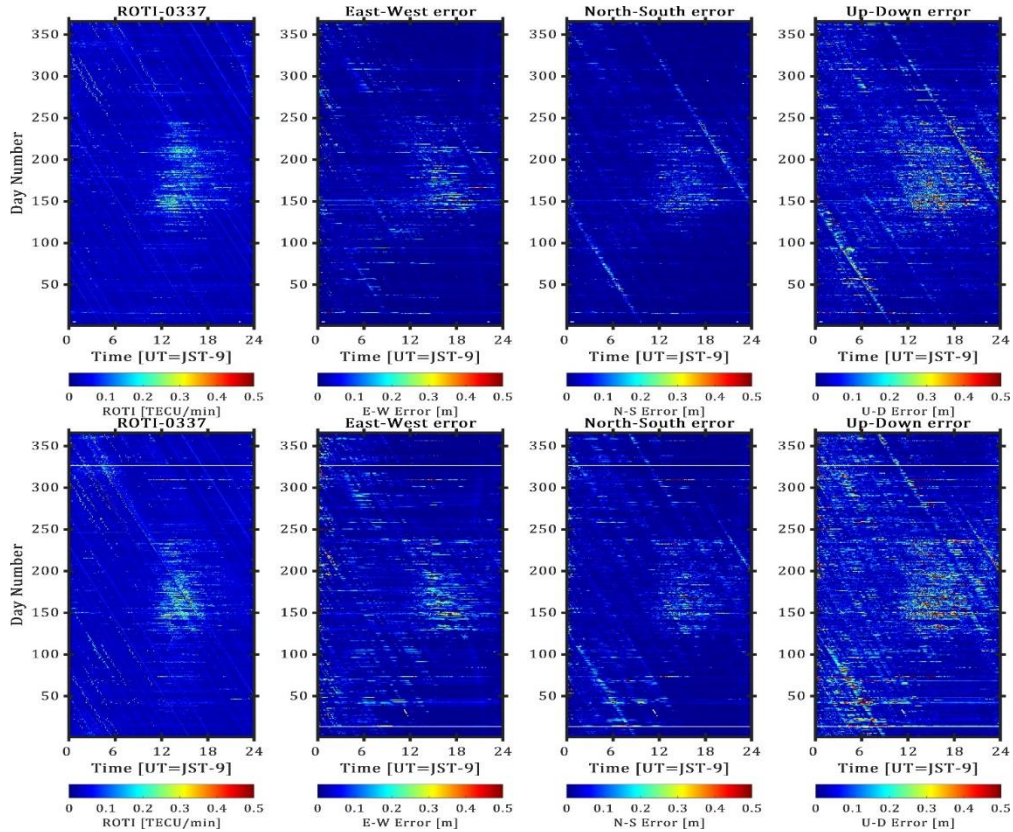


Figure 2: Day-to-day variation of ROTI and associated positioning errors observed at station 0337 in region 3 during the period spanning 2022 (top panel) to 2023 (bottom panel).

Period of Stay at ISEE, Nagoya University: 26 November 2023 to 19 February 2024

Paper Submitted in JpGU 2024 for Oral Presentation: Rajesh Kumar Barad, Y. Otsuka, S Sripathi, P. Abadi, A. Shinbori, T. Sori, M. Nishioka, and P. Septi, Characterizing the Effects of Mid-Latitude MSTIDs on GNSS Positioning Accuracy Across Japan Using a Dense Receiver Network (**Abstract accepted**)

Occurrence of red-green low latitude aurora during large geomagnetic disturbances: Case studies

Manu Varghese, ISS, Shandong University, Weihai, China; Research Student

Personal Note

Fortunate to have been associated with the Institute of Space Earth Environment (ISEE) at Nagoya University, Japan, under the supervision of Prof. Kazuo Shiokawa when I was awarded the prestigious SCOSTEP Visiting Scholarship to conduct a research project during October-December 2023.

Space Physics Context

Auroras are observed and studied using ground and space based instruments over decades. Space based observations reveal the large-scale evolution of auroras, but the fine structures are not evident. On the other hand, fine structures are clear from the ground observations but are sometimes limited by the cloudy skies and moonlight. Auroras at mid-low latitudes are observed over centuries (e.g., Loomis, 1861; Chapman, 1957; Tinsley et al., 1986; Rassoul et al., 1992; Miyaoka et al., 1990; Shiokawa et al., 1994). During high geomagnetic activity, auroral oval expands to lower latitudes. The important driving mechanisms for low latitude auroras are broadband electrons and stable auroral red (SAR) arcs. Observations have shown that these auroras have red to green emission ratio greater than 10, and the dominant red emissions are caused by the de-excitation of atomic oxygen mainly in the top side ionosphere. The north looking all sky cameras from Japan usually observe the red aurora during the main phase of geomagnetic storms and with storm-time substorm activity. The electron precipitations over a wide energy range, 30 eV – 30 KeV were reported from earlier DMSP observations during such substorms (Shiokawa et al., 1997). Stable Auroral Red (SAR) arcs formed in sub auroral latitudes also cause low latitude auroras, which are during the recovery phase (RP) of geomagnetic storms. SAR arcs last more than 10 hours and are caused by low energy electron precipitation (<10 eV). SAR arcs occur due to the Coulomb collision between energetic ring current ions and the electrons in the plasmasphere causing precipitation to sub-auroral latitudes.

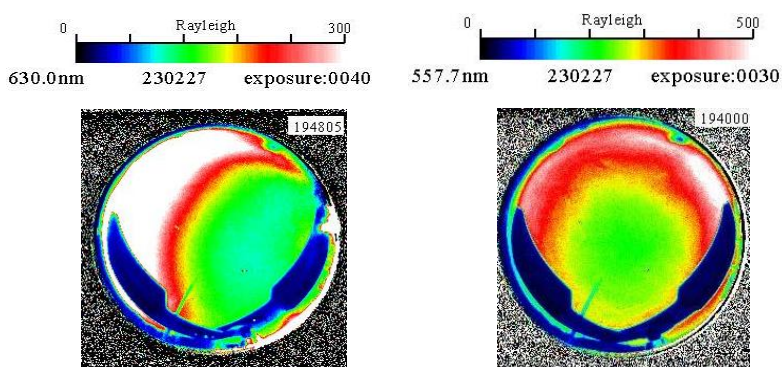


Fig 1: Red and green aurora from Rikubetsu at ~19:45 UT on 27 February 2023

Only a limited number of low latitude auroras were reported, mostly red emissions and at high levels of solar activity. Recently, unusual red and green simultaneous auroral emissions of comparable intensities are observed from Rikubetsu, Japan (43.5° N magnetic latitude) during the rising phase of solar cycle 25. One such red-green aurora of ~300-400R are observed during the geomagnetic

storms on 27 February 2023. Detailed investigations of these events are made to understand their dynamics.

Data Analysis and Methodology

The primary observations are based on All sky camera and photometer measurements from Rikubetsu, Japan (43.5 N, 143.8 E, magnetic latitude) which is a contributing station in the OMTI network (Shiokawa et al.,

1999, 2000). The electron precipitation, density and temperature data are from DMSP, NOAA/POES METOP and SWARM satellites.

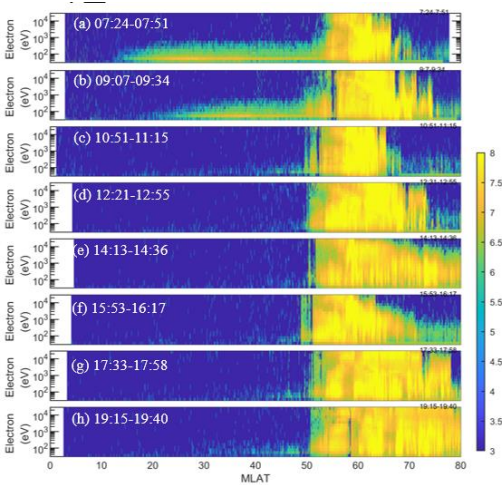


Fig 2: DMSP F18 shows the auroral expansion

Results

Low Latitude Aurora on 27 February 2023

This aurora (Fig. 1) is seen (16:00-20:00 UT) during the RP of a storm with prior SymHMin of -160 nT at 12 UT. The solar wind velocity increases to ~850 km/s and IMF Bz to -20 nT indicating the possibility of strong magnetosphere-ionosphere coupling. DMSP F18 satellite close to the time and location of the aurora recorded the auroral oval expansion to ~48° mag. lat. (Fig. 2). The temperature increased with the corresponding decrease in density indicating the development of SAR arcs.

Stay at ISEE, Nagoya University

My time in Nagoya was very pleasant and perfect both for research and living with sports and cultural activities. The weekly discussions with Prof. Shiokawa and his lectures on plasma dynamics to the master students gave me insights into the way of delivering knowledge, sharing ideas, and mentoring. His association significantly increased my understanding of the behaviour of plasma in the solar wind, magnetosphere, and ionosphere.

Though it was a short stay, I could carry a bag full of treasured memories ranging from the futsal matches every week with professors and students to the calm brainstorming discussions. Fondly acknowledging and thanking Dr. Kazuo Shiokawa, Dr. Yuichi Otsuka, Dr. Claudia Martinez, Dr. Shreedevi P. R, Dr. Abadi Prayitno, Mr. Rei Sugimura, Mr. Gomi Masaki, Ms. Miho Sugiyama, and Ms. Naoko Kashimura for all the academic and administrative assistance.



Large scale changes in the polar ionosphere during CME and CIR storms, its relation to Sub-Auroral Polarization Streams (SAPS) and particle precipitation

Ardra Kozhikottuparambil, PhD Scholar

Centre for Fusion, Space and Astrophysics (CFSA), University of Warwick, UK

Purpose of research: Sub Auroral Polarization Streams (SAPS); encompass various phenomena like Polarization Jets (PJ), Subauroral Ion Drifts (SAID), subauroral electric fields, auroral westward flow channels, and radar auroral surges. These occur in a sunward plasma channel below the auroral oval during geomagnetic storms. SAPS involves poleward-directed electric fields in the plasma spheric boundary layer, affecting storm-time phenomena like storm-enhanced density/plasma spheric plumes and density troughs in the midlatitude ionosphere. It erodes plasma content, transporting it to the dayside noontime cusp, resulting in space weather effects observed in the midlatitude ionosphere.

Early observations linked SAPS to substorms, but recent studies reveal their permanent presence during geomagnetic activity with varying intensity and spatial extent. Initial understanding relied on statistical studies using DMSP satellites and Millstone Hill radar. Later, SuperDARN measurements shed light on the influence of magnetosphere-ionosphere dynamics, interhemispheric magnetic conjugacy, and geomagnetic conditions on SAPS.

Studies using magnetically conjugate observations have proposed that the broad SAPS channel and the other phenomena grouped within it may have different driving mechanisms, thereby challenging our previous understanding of their evolution. This evolving field is due to past studies mainly focusing on individual event periods driven by Coronal Mass Ejections (CMEs). Our proposed research aims to compare SAPS features during CIR and CME-driven geomagnetic storms to better understand their distinctive nature and characteristics.

Methodology:

Phase 1: Classification of storms based on their drivers

The geomagnetic conditions during the selected events were obtained using the solar wind and magnetic field measurements from the ACE and WIND satellites (<https://cdaweb.gsfc.nasa.gov/>). The datasets obtained from the ACE and WIND satellites were used to identify the solar wind drivers into CMEs and CIRs. The Dst index, employed to represent the intensity of geomagnetic storm, was obtained from the World Data Centre, Kyoto (<http://wdc.kugi.kyoto-u.ac.jp>).

Phase 2: Study and validation using datasets.

DMSP observations were used to analyze particle precipitation and SAPS characteristics. Accurate identification of SAPS events depended on precise auroral oval location data. The SSJ/4 instrument on DMSP satellites determined SAPS boundaries. Data was sourced from the Cedar Madrigal database (<http://cedar.openmadrigal.org/>). Substorm activity was evaluated using AE and AL indices from <https://omniweb.gsfc.nasa.gov/ow.html>.

Convection was studied with SuperDARN velocity measurements and GPS-TEC data from Nagoya University (<https://stdb2.isee.nagoya-u.ac.jp/GPS/GPS-TEC/>). AMPERE satellite field-aligned currents were incorporated for a detailed comparison with plasma density evolution during CIR and CME events. AMPERE data can be found at <https://ampere.jhuapl.edu/>.

Results and Conclusion: The analysis of the evolution of SAPS (Subauroral Polarization Streams) from both CME (Coronal Mass Ejection) and CIR (Corotating Interaction Region) driven storms reveals distinct trends. CME-driven storms tend to be intense but of short duration, whereas CIR-driven storms are characterized by their prevailing nature, albeit with lower intensity. Furthermore, there is a noticeable seasonal variation in these patterns in the respective hemispheres. Fig. 1 shows DMSP observations of the event on 8th June 2015, which clearly shows the interhemispheric asymmetry in the zonal velocities. This study also indicates a strong correlation between SAPS and geomagnetic indices like AE (Auroral Electrojet) and AL (Auroral Electrojet Index, indicating the Lower envelope of the north-south magnetic field variations), further emphasizing the interplay of these phenomena in the Earth's magnetosphere.

The SuperDARN convection maps exhibited strong correlations with the observed convection patterns from DMSP and GPS TEC data. The line-of-sight velocity distributions effectively depicted the convection directions during the storm period. Fig. 2(a) and 2(b) show the line-of-sight velocity distributions and convection obtained from SuperDARN radars for the northern and southern hemispheres validating the DMSP observations.

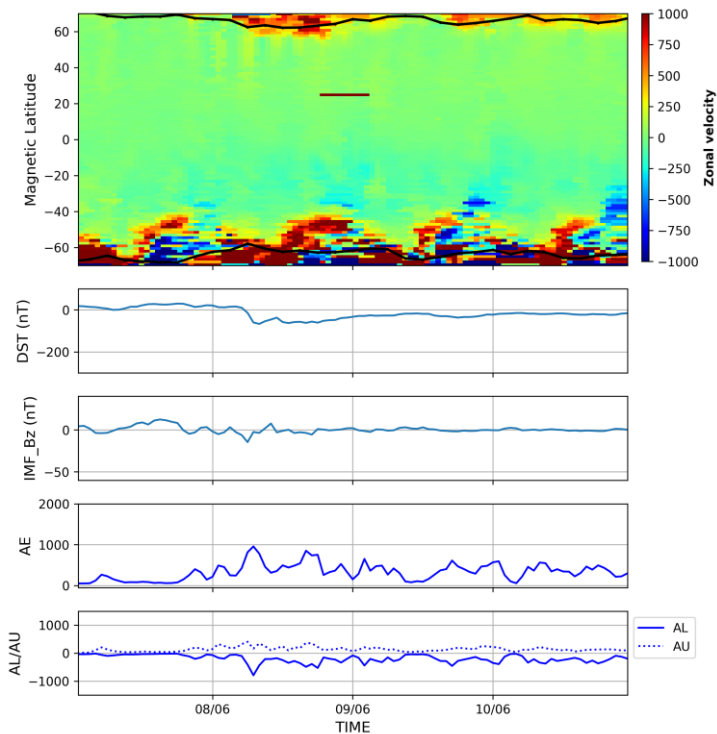


Fig 1. In a geomagnetic storm in June 2015, Subauroral Polarization Streams (SAPS) are observed. The top panel shows residual zonal velocity data from the F16 satellite. The black line indicates the equatorward boundary of the auroral oval, taken from the auroral boundary index. The second and third panels display the temporal evolution of Dst and IMF Bz. The third and fourth panel shows the AE and AL/AU.

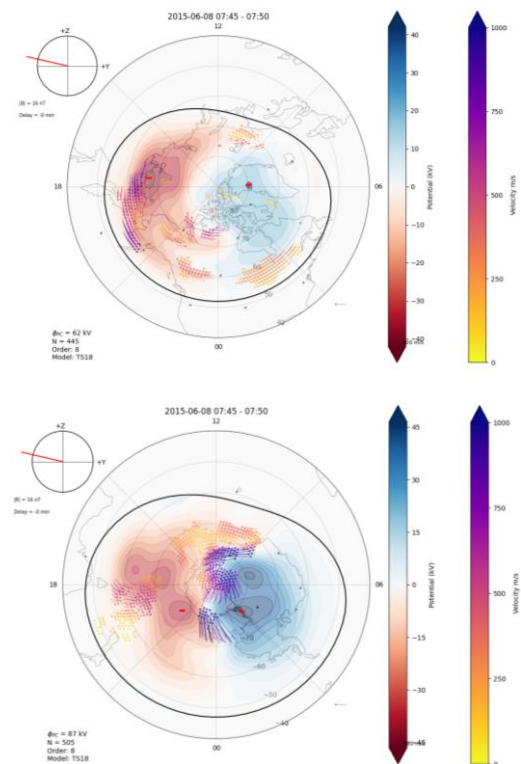


Fig 2(a). (top) and Fig 2(b). (bottom) shows the line-of-sight velocities and convection map obtained from SuperDARN radar observations for 8th June 2015 in the northern and southern hemispheres respectively between 07.45-07.50 local time.

Future work: In the next phase, the research will encompass a comprehensive analysis of almost all storms occurring between 2015 and 2023. This will involve integrating AMPERE (Active Magnetosphere and Planetary Electrodynamics Response Experiment) data with the existing DMSP, SuperDARN, and GPS-TEC observations. The main objective of this endeavour is to compile and publish a paper on this subject in a reputable academic journal.

Period of stay at ISEE: 11th June 2023 to 20th August 2023

References:

- [1] A. Coster and J. C. Foster. Space-Weather Impacts of the Sub-Auroral Polarization Stream. *Radio Science*, (321), 2007.
- [2] J. C. Foster. Ionospheric-Magnetospheric-Heliospheric Coupling: Storm-Time Thermal Plasma Redistribution. *Geophysical Monograph Series*, 181, 2008.
- [3] G. W. Pröls. Ionospheric F-region storms. In :H., Volland (Ed.), *Handbook of Atmospheric Electrodynamics*, 2:195–248, 1995.
- [4] W. D. Gonzalez, B. T. Tsurutani, and Alicia L. Clua De Gonzalez. Interplanetary origin of geomagnetic storms. *Space Science Reviews*, 88:529–562, 1999.
- [5] Nishitani, N., Ruohoniemi, J.M., Lester, M. et al. Review of the accomplishments of mid-latitude Super Dual Auroral Radar Network (SuperDARN) HF radars. *Prog Earth Planet Sci* 6, 27, 2019
- [6] P. R. Shreedevi, S. V. Thampi, D. Chakrabarty, R. K. Choudhary, T. K. Pant, A. Bhardwaj, and S. Mukherjee. On the latitudinal changes in ionospheric electrodynamics and composition based on observations over the 76–77°E meridian from both hemispheres during a geomagnetic storm. *J. Geophys. Res. Space Physics*, 121, 2016.
- [7] Y. Galperin, V. Ponomarev, and A. Zosimova. Plasma convection in the polar ionosphere. *Annales Geophysical Research*, (30):1–7, 1974.
- [8] J. C. Foster and W. J. Burke. SAPS: A New Categorization for Sub-Auroral Electric Fields. *Eos, Transactions American Geophysical Union*, 83(36):393–394, 2002.
- [9] Joseph E. Borovsky and Michael H. Denton. Differences between CME-driven storms and CIR driven storms. *Journal of Geophysical Research: Space Physics*, 111(A7), 2006. A07S08.
- [10] B. S. R. Kunduri, J. B. H. Baker, J. M. Ruohoniemi, N. Nishitani, K. Oksavik, P. J. Erickson, A. J. Coster, S. G. Shepherd, W. A. Bristow, and E. S. Miller. A new empirical model of the subauroral polarization stream. *Journal of Geophysical Research: Space Physics*, 123(9):7342–7357, 2018.
- [11] P. C. Anderson, D. L. Carpenter, K. Tsuruda, T. Mukai, and F. J. Rich. Multisatellite Observations of Rapid Subauroral Ion Drifts (SAID). *Journal of Geophysical Research: Space Physics*, 106(A12):29585–29599, 2001.